Robust Multi-Scale Orientation Estimation: Spatial domain Vs Fourier domain

Mohammad A. U. Khan
Electrical and Computer Engineering Department
Effat University
P.O.Box 34689
Jeddah 21478
Saudia Arabia
TEL : +966-2-6364300
FAX : +966-2-6377447
Email: makhan@effatuniversity.edu.sa

Wadee Alhalabi
Computer Science Department
Effat University
P.O.Box 34689
Jeddah 21478
Saudia Arabia
TEL : +966-2-6364300
FAX : +966-2-6377447
Email: walhalabi@effatuniversity.edu.sa

***Abstract*—Orientation estimation is considered as an important and vital step towards many pattern recognition and image enhancement tasks. In a noisy environment, the gradient-based estimations provide poor results. A pre-smoothing Gaussian function with an appropriate scale is conventionally used to get better gradients. Later on, fixed-scale approach was extended to include multi-scale gradient estimates. More specifically, multi-scale orientation estimation, based on scale-space axioms, in spatial domain can be formulated. To further boost the performance of multi-scale orientation estimates, a Fourier domain foundation in the form of Directional Filter bank (DFB)is incorporated with multi scale spatial domain approach. This paper presents an approach for estimation of local orientations using multi-scale approach both in spatial and fourier domain. In fourier-domain approach, two linear combinations are deployed, one across the directional image, and the other across scales. This is opposed to only one linear combination across the scales, used in normal spatial domain technique. Simulations are conducted over noisy test images as well as real data. Our objective results indicate that multi-scale fourier domain approach always yields better estimates at variable level of noise as compared to stand alone multi-scale spatial domain. The improvements made by fourier domain estimate can largely be attributed to the use of double linear combination both across directional bands and across scales.**

I. Introduction

Orientation Field (OF) estimation is considered to be challenging task, particularly in the presence of noise. Once reliably extracted this orientation filed can be utilized in a number of ways to enhance the quality of the features to be detected in a given image. The motivation for the desire to extract reliable orientation filed came from our previous work on angiogram image enhancement task [4], where a two-dimensional non-linear diffusion process put forth in [1] for enhancement was found to be conveniently decomposed as a separable two one-dimensional diffusion process once we know local orientations, where one process goes along the features and the other to go across it. Motivated by their use in simplifying the enhancement process, we focus here on robust estimation of the orientation fields in noisy images.

The most natural tool for finding orientations at location (x, y) of an image f, is the gradient, denoted by ∇f, and defined as the vector

$$\nabla f \equiv \begin{pmatrix} g_x \\ g_y \end{pmatrix} \quad (1)$$

The vector has the geometrical property that it points in the direction of greatest rate of change of f at location (x, y). The orientations can be defined as $\theta(x, y) = \frac{\pi}{2} + \arctan[\frac{g_y}{g_x}]$ measured with respect to the x-axis. The images, acquired from sensors, are usually noisy, making the job of extracting local orientation hard. One effective way to reduce the effect of noise is to smooth the image before taking derivatives. For this purpose, a 2-D Gaussian function $G(x, y) = e^{-\frac{x^2+y^2}{2\sigma^2}}$ is employed with a specified scaleσ. The scale associated with Gaussian function has to related with features present in the images. This give rise to Scale-space theory [12], which suggest to use variable scales for different features. Here, we looked towards Scale-space theory for guidance to provide a unified framework for selecting appropriate scales for effective and reliable local orientation estimations.

A simple but elegant regularization step was proposed by Kass & Witkin in [2], which allows local gradient estimates to be averaged. They introduced the idea of doubling the orientation angles and averaging the angles in a local $n \times n$ window with x- and y-component treated separately. In the mean time, the idea of orientation diffusion was also floated [15].However, the orientation diffusion on average takes large number of iterations to converge. Later on, the authors in [5] shown that based on the above idea, an effective method for computing the orientation filed of a fingerprint image can be derived. The derived method is mathematically equivalent to taking the principal component analysis of autocorrelation matrix of the gradient vectors in a local neighborhood. Building upon this, a PCA-based method in a multi-scale framework was

978-1-4673-2821-0/13/ $31.00©2013 IEEE

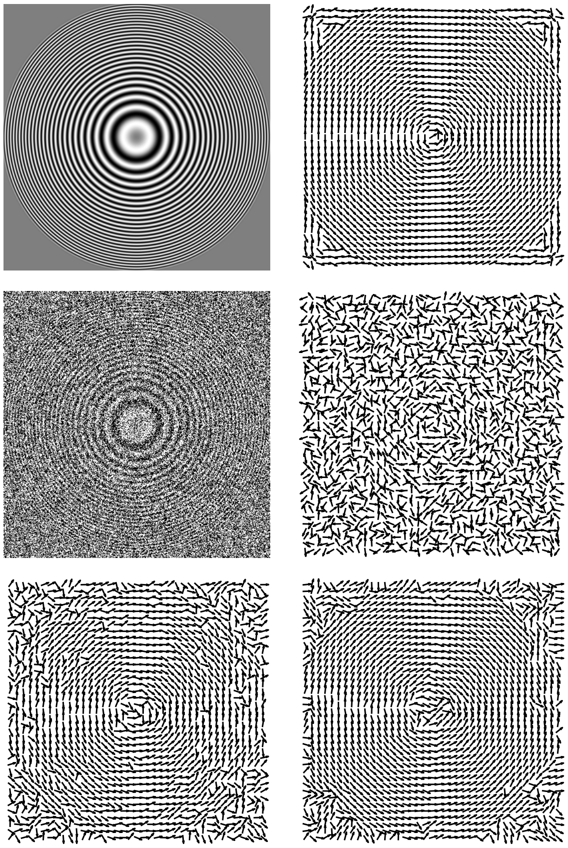

Fig. 1. Orientation Estimation-The figures on the top row shows the test image, along with its true directions. The second row shows the noisy test image with its fixed-scale gradient-based orientation estimation on the right. The third row depicts the performance of multi-scale spatial domain on the left, and multi-scale fourier domain on the right.

introduced in [3] which effectively enforced smoothness across scales. Since the method works in a multi scale environment, it provides a compromise between native resolution of the orientation field and its relative accuracy. The PCA analysis is applied to find the maximum likelihood (ML) estimate of the local orientation by finding the optimal local neighborhood. Though the multi-scale PCA technique is shown to produce robustness against noise, its performance suffers as the amount of noise increases. For noisy environment, reliable orientation estimates can be obtained in the Fourier domain [8]. Another recent article [7] proposes the use of parallel neighboring cells to improve the local estimate. However, the size of the neighborhood is fixed for all the pixels under consideration. In the same vein, a reliable orientation estimate is also put forth in [9]. However, all these methods deal in one way or the other with the spatial domain enhancements. In this paper, we present the compromise between native resolution of local orientation estimate and the degree of accuracy in the Fourier domain.

There are a few fixed-scale transform domain orientation estimation techniques reported in literature. A curvelet-based method for local orientation is introduced in [10], where a *mother curvelet* is scaled and rotated to find the optimal local orientation. However, the method is strictly fixed-scale with assumption of knowing the object size. Another Fourier-based technique is demonstrated with finding the fiber orientation of a paper surface [11]. Here Fourier transform of the image is taken and then converted to polar co-ordinates. The power spectrum is radially accumulated along various orientation. The orientation of the paper is announced with maximum accumulation along a given orientation. This method provided global orientation of a given paper image. Considering a texture image as a combination of piecewise linear components, a directional filter bank approach has been successfully used in enhancing weak features [4]. Specifically, the input image is first decomposed using a Decimation-free Directional Filter Bank (DDFB), referred to as DFB in the remainder of the paper, into a set of directional images, each of which contains linear features in a narrow directional range. The directional decomposition has one main advantage. The directional images, as output of DFB, contain only features in a narrow directional band and are found to contain significantly less noise as compared to the original image. The suppression of noise in directional images facilitates the computation of gradients. However, the gradient computation for declaring a local orientation among directional images is performed within a fixed block/scale. Thus, essentially it constitutes a fixed-scale DFB-based fingerprint orientation calculation and pretty much restricts its capability for noise suppression.

In order to incorporate DFB for multi scale orientation estimation, we first create a coarse orientation estimate for each directional image and then average them across the bands as well as across the scales. This provides us with extra capability of adaptively changing the scale within the DFB framework to obtain an optimal orientation estimate with the characteristics of noise robustness and feature localization.

Fig. 1 shows a three-row array of pictures for comparison purposes. The first row displays the test image used for assessing the performance of spatial as well as fourier domain approaches. The gradient-based approach is working fine with the noise-free test image. However, we observe that from the second row, that its performance degrades with the noisy data. The third row depicts the performance of spatial as well as fourier domain approaches for the noisy test image. The multi-scale spatial and fourier domain does a better job at extracting directions. The fourier domain orientation estimation is clearly doing an improved job over that of spatial domain, with the average absolute angle error of approximately $\frac{\pi}{15}$ as compared to $\frac{\pi}{10}$ for that of spatial domain. Besides, we also observe in Fig. 1, a critical limitation of the proposed multi-scale DFB approach in the center of the test image. Since the center contains sharp turns, the fourier domain approach was not able to effectively represent these sharp turns as piece-wise linear segments.

The paper is organized as follows. Section A explains the multi-scale spatial domain method. Multi-scale DBF based orientation estimation is proposed in section B. Simulation results and objective quality measure are discussed in Section C. Finally, Section D presents our concluding remarks.

A. Multi-Scale Spatial domain method

For the sake of orientation estimation, the covariance matrix is formed by gradient vectors in a local square window of width n, as described below.

$$C = \begin{bmatrix} \sum_{i=1}^{n} g_{i,x}^2 & \sum_{i=1}^{n} g_{i,x} g_{i,y} \\ \sum_{i=1}^{n} g_{i,x} g_{i,y} & \sum_{i=1}^{n} g_{i,y}^2 \end{bmatrix}, \quad (2)$$

where $g_{i,x}$ and $g_{i,y}$ are derivatives in x and y direction at pixel location indexed by i, respectively. The Principal Component Analysis (PCA) of the covariance matrix provides the eigen vectors and their eigen values. The image orientation can be obtained from the eigen vectors of the matrix C. The eigen values associated with their corresponding eigen vectors represent the square root of the energy in corresponding principal directions. The orientation estimation can be improved upon by setting it in a multiscale framework [13]. The multi scale model describes images in terms of an evolution from coarse to fine scales, and is also more similar to the human visual system. The major problem of the orientation estimation is the noise sensitivity of the gradient operator. In order to depress the noise effect, one solution is using larger estimate window, since more neighboring gradients will be used to get the estimate and the averaging process will depress or eliminate the noise effect all together. But this will cause the loss of the estimate resolution. A mechanism with both noise robustness and feature localization is needed. Multi scale model provides an efficient way to combine the information from coarse scales and fine scales. The multi scale approach can be used to obtain Minimum Mean Square Error (MMSE)estimate, which is based on a Kalman filter-like multi scale model, introduced in [5].

A Multi-scale spatial domain approach for orientation estimation is formulated in this research as follows. Given an input image $f(x, y)$, this image is convolved by a Gaussian kernel $g(x, y; t) = \frac{1}{2\pi t^2} e^{\frac{-(x^2+y^2)}{2t}}$ at a scale t , the parameter t is equal to the square of the standard deviation σ, to give a scale-space representation $L(x, y; t) = g(x, y; t) * f(x, y)$. Then for each scale-space image $L(x, y; t)$, we compute the second-order partial derivatives in the form of the Second Moment Matrix, as follows.

$$H(x, y; t) = \begin{bmatrix} L_x^2 & L_x L_y \\ L_x L_y & L_y^2 \end{bmatrix}, \quad (3)$$

where L_x represents the first-order partial derivative of the scale-space image $L(x, y; t)$ with respect to x-axis, L_y represents the first-order partial derivative of the scale-space image $L(x, y; t)$ with respect to y-axis. This four-element matrix is computed for each pixel of the scale image. This symmetric positive-definite matrix can be decomposed using eigen values analysis. We get two eigen values λ_{min} and λ_{max}, with associated eigen vectors $\mathbf{e_1}$, depicting direction along the texture, and second eigen vector $\mathbf{e_2}$, corresponding to the direction normal to the texture at that pixel.

Experiments show that the scale parameter of the Gaussian pre-smoothing kernel t must be carefully tuned to the width of the directional feature present in a given image. The eigen vector $\mathbf{e_{2,t}}$ calculated at a given scale t will provide the texture orientation at a pixel location in the form $\theta(x, y; t) = \arctan(\frac{e_{2,t,y}}{e_{2,t,x}})$. Next we take the multi-scale measure of scale-space texture representation as suggested in [6], [14], defined as

$$A(x, y; t) = t^{\frac{3}{2}} (\lambda_{max} - \lambda_{min})^2, \quad (4)$$

for each pixel location. In this way we computed the orientations and their strength measure for the whole family of the scale-space images. To estimate the most likelihood orientation, we first decompose the eigen value $e_{2;t}$ into its orthogonal components, that is $e_{2,x;t}$ and $e_{2,y;t}$. Then for each pixel location, the final orientation estimate is computed as linear combinations of these orthogonal components with their respective strength measures as described below.

$$\begin{aligned} X &= \frac{A(x,y,1)}{\sum_{t=1}^{N} A(x,y,t)} e_{2,x;1} + \frac{A(x,y,2)}{\sum_{t=1}^{N} A(x,y,t)} e_{2,x;2} \\ &+ \cdots + \frac{A(x,y,N)}{\sum_{t=1}^{N} A(x,y,t)} e_{2,x;N}. \end{aligned} \quad (5)$$

Similarly, we computed the Y part of the orientation estimate. Next, final orientation estimate for the whole image is computed as $\arctan \frac{Y}{X}$. While implementing the algorithm, we are in need of scale range to be used for a given image. The process of selecting the scale range can be automated. We adopted a similar approach as described in [12]. We constructed a scale space by convolving image with Gaussian having progressively increasing standard deviation taken as scale parameter. Then, for each scale image, we computed the average of following normalized coherence measure, as described in [12].

$$S_{norm} L = t^{\frac{1}{2}} (L_x^2 + L_y^2) + \frac{2}{3} t^{\frac{3}{2}} ((L_{xx} - L_{yy})^2 + 4L_{xy}^2) \quad (6)$$

The t represents the scale parameter, $L_x$andL_{xx} denoted the first- and second-order partial derivative of the image in x direction. Similarly. $L_y$andL_{yy} show the partial derivatives in the y direction. The measure provides maximum for a given average local scale, t_{local}. The scale range can then be safely selected as a set that initiates with scale $\frac{t_{local}}{4}$ and ends with scale $4t_{local}$.

B. Multi-scale Fourier Domain Approach

In order to embed the DFB structure with the multi-scale spatial domain approach discussed earlier, we adopted the following procedure.

Step 1An image $f(x, y)$, in which directional texture can be modeled as piece-wise linear segments, is first convolved with a smoothing Gaussian of a given scale, to form a scale-space image.

Step 2 The scale-space image is then decomposed using Directional Filter bank in a number of directional images $f(x, y; i)$, where $i = 1, 2, \cdots, n$ corresponds to the orientation associated with each directional image in the range $\theta_1, \theta_2, \cdots, \theta_n$.

Two directional images are displayed in Fig. along with their associated energy measures. We observe that directional images are fairly concentrated in a narrow angular width, in this case it is $\frac{\pi}{16}$, and the energy images are also representative of their strength measures.

Step 2 For each pixel location, the directional information present at directional images need to be linearly combined. That is what we usually do in the conventional setup. However, due to the presence of local noise, it is proposed that this job of linear combination across the directional images should be set in the scale-space framework.

Therefore, we first define a set of scales as $t \in 1, 2, \cdots, N$. Then, to measure the strength associated with a given directional image, we define its strength measure same as that in the previous section, that is $A(x, y; i, t)$, where i represents the direction θ_i and t represent the scale chosen. The strength calculation can be mathematically defined as

$$A(x, y; i, t) = t^{\frac{3}{2}} (\lambda_{max})^2. \quad (7)$$

Step 3 Now, the directional information available to use through directional image θ_i are linearly combined using accumulated strength measures at each pixel across its directional images. This ends up in an orientation image at a given scale t. Let us call it $O(x, y; t)$. That is,

$$O(x, y; t) = \sum_{i=1}^{n} \frac{A(x, y; i, t)}{\sum_{i=1}^{n} A(x, y; i, t)} \theta_i. \quad (8)$$

Step 4 Then, having a whole family of $O(x, y; t)$ and strength images defined at each pixel location and scale as $S(x, y; t) = \sum_{i=1}^{n} (x, y; i, t)$, we are in a position to repeat the process of linear combination again, but this time across the scales. This provided us with a final robust estimate $\theta_{final}(x, y)$ of the orientation image. That is,

$$\theta_{final}(x, y) = \sum_{t=1}^{N} \frac{S(x, y; t)}{\sum_{t=1}^{N} S(x, y; t)} O(x, y; t). \quad (9)$$

C. Results and Discussions

In order to assess the quality of the proposed multi-scale orientation estimate over that of single-scale approach, we tested the approach for a synthetic test image, referred to as Jahne's pattern [16]. The mathematical expression governing the pattern is depicted as:

$$g(\mathbf{x}) = g_0 \sin(\frac{k_m |\mathbf{x}|^2}{2 r_m}) \left[\frac{1}{2} \tanh(\frac{r_m - |\mathbf{x}|}{w}) + \frac{1}{2} \right], \quad (10)$$

where r_m is the maximum radius of the pattern, $\tanh(\frac{r_m - |\mathbf{x}|}{w})$ as an approximation to a step function with a as the location of the step and w is the width of the transition. We set the parameters so that the maximum instantaneous frequency of $k_m = 0.5\pi$ is reached in the center of the image edges, and then the tapering function prevents aliasing artifacts from appearing as we move out to the corners. The pattern as shown in Fig. is displayed on a grid 400×400. The test image with and without noise is shown in Fig. 1.

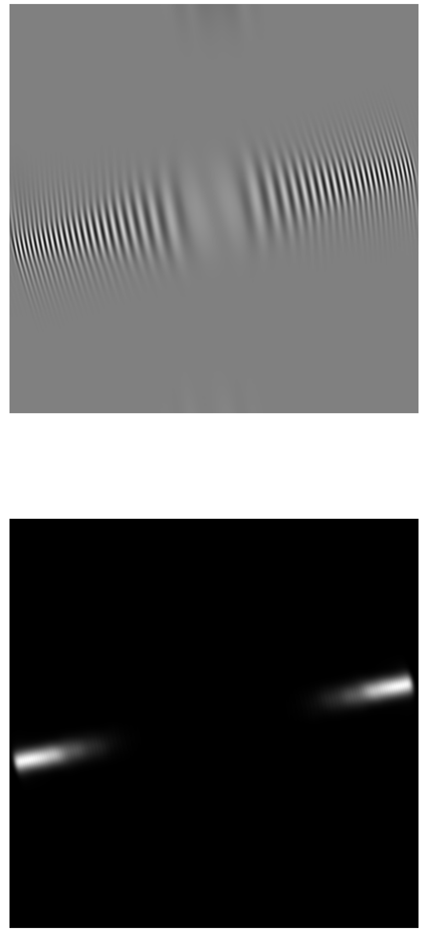

Fig. 2. Creation of Directional Images: The top figure shows third directional image out of total 32 bands uniformly distributed over the range from $-\pi$ to π and its associated strength below.

The MATLAB gradient functions are used to compute the numerical gradients in x and y directions. Then MATLAB arctan function is invoked to compute the true orientation field of the test image as depicted in first row right in Fig.1. The ground truth orientations for the test image can be calculated as $\theta(x, y) = \arctan(\frac{f_y(x,y)}{f_x(x,y)})$. Now we will add Gaussian noise of zero mean and variance that increases progressively in the test image. These noisy test images are then presented to both, the single-scale PCA and multi-scale approaches to assess their performances. we use scales that range from 0.5-6. For defining the objective criterion, we use the absolute angle difference in radian. The pixel-wise angle error can be defined as

$$E(\theta_{estimated}, \theta_{original}) = |\theta_{estimated} - \theta_{original}|. \quad (11)$$

The performance of multi-scale fourier approach is also

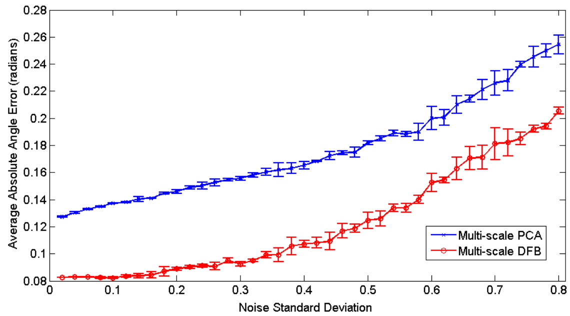

Fig. 3. The graph showing the comparison of multi-scale spatial domain orientation estimate with that of multi-scale fourier domain. The curves are drawn as average angle error in radian against the increasing value of noise variance.

compared with multi-scale spatial technique as a function of noise variance. We see from the Fig. 3 that the fourier domain error is all times less than that of spatial domain and as we move towards the higher noise variance the fourier domain curve maintains a constant advantage over that of spatial domain. The curve plotted here are the average of 100 runs of random noise generators with 100 different seed points.

In another set of experiments, we investigated the impact

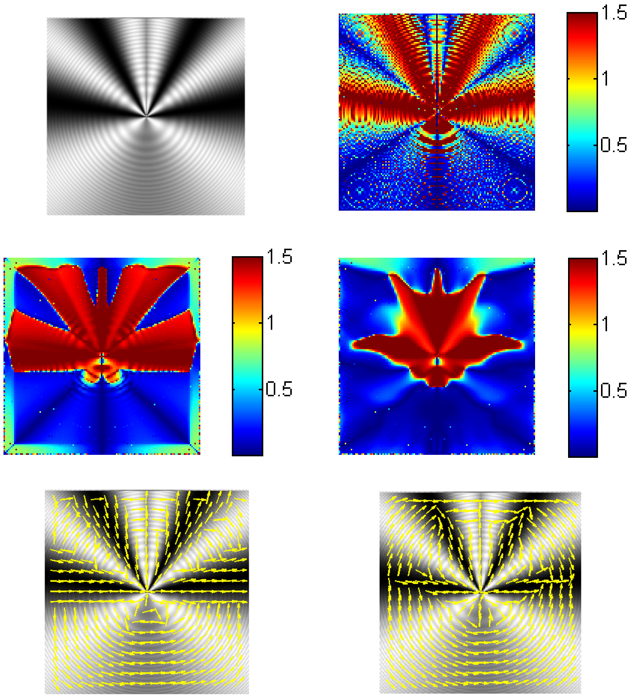

Fig. 4. The Effect of Contrast: The Top row-Left is a test image synthesized as a pixel-wise multiplication of a sinusoidal contrast variation interference pattern as we move around the image center and our ground truth image having concentric circle pattern. The Top row-Right is the result of absolute orientation error image using gradients. The second row-left is the error image due to multi-scale spatial approach. The second row-right is the orientation error image due to the proposed multi-scale fourier technique. The third row-left is the orientation filed due to multi-scale spatial and third row-right is the multi-scale fourier based orientation filed for the test image.

of contrast on the robustness of the proposed local orientation estimation. A test image is synthesized by pixel-wise mul-

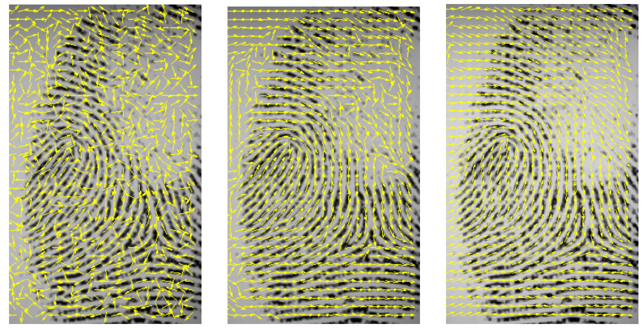

Fig. 5. Real Fingerprint Images: The performance of the gradient technique, multi-scale spatial and that of multi-scale fourier domain for the real fingerprint image taken from the international fingerprint database NIST. We observe the consistent behavior of the proposed multi-scale DFB for the noisy regions. The CPU time noted for a Pentium 4 machine with 2 GHz, for the gradient approach is 0.43 seconds, for multi-scale spatial domain is 1.5 seconds and that for the multi-scale fourier domain is 3.1 seconds.

tiplication of our ground truth concentric circle image with amplitude 0.01 and an interference pattern having periodic dark and white regions with amplitude 0.5. The product results in a test image where contrast is varying as move on the image from one pixel location to the next. The interference image is synthesized as follows,

$$f(x, y) = \sin(\theta), \tag{12}$$

where $\theta = \arctan(\frac{y}{x})$. Since true orientations are available for the ground truth, we compare the strength of our proposed technique with that of multi-scale PCA and the gradient-based approach. The absolute angle error is displayed in a color-coded manner. The Fig. 4 shows that the fourier method does a fairly good job of tracking the true orientations even in dark regions of the test image to some extent.

The proposed spatial and fourier domain estimations was also tested on the real fingerprint images from NIST database publicly available. We observe that fourier domain orientation estimation provides improve flow directions, consistent with the human expert predictions. The Fig. 5 reveals the fingerprint orientation fields for the three methods.

D. Concluding Remarks

This paper presents the extension of multi-scale PCA to that of Fourier domain. A robust algorithm is presented that incorporates Directional filter bank images as foundation for applying multi-scale PCA. Experiments were conducted on test images with true orientation known. It was suggested with the objective criterion that fourier domain multi-scale will provide better results for orientation estimation in noisy environment over that of multi-scale spatial domain. This robustness can be attributed to the presence of two-dimensional linear combination, where one that goes across the directional images and then across the scales. This attribute was found effective in combating the local noise present without disturbing the flow directions in a given image.

References

[1] A. Almansa and T. Lindberg, "Fingerprint Enhancement by Shape Adaptation of Scale-Space Operators with Automatic Scale-Selection," *IEEE Trans. on Image Processing*, vol. 9, no. 12, pp. 2027-2042, 2000.

[2] M. Kass and A. Witkin, “Analyzing Oriented Patterns,” *Computer Vision, Graphics, and Image Processing*, vol. 37, no. 3, pp. 362-385, 1987.

[3] , X. G. Feng and P. Milanfar, “Multiscale principal components analysis for image local orientation estimation,” *Conference Record of the Thirty-Sixth Asilomar Conference on Signals, Systems and Computers, 2002*, California, USA,3-6 Nov, pp. 478-482,2002.

[4] P. T. H. Truc and M. A. U. Khan and Y. K. Lee and T. S. Kim”, “Vessel enhancement filter using directional filter bank”, *Computer Vision and Image Understanding*, vol. 113, issue 1, pp. 101-112, 2009.

[5] A. M. Bazen and S. H. Gerez”, “Systematic Methods for the Computations of the Directional Fileds and Singular Points of Fingerprints”, *IEEE Trans. on Pattern Analysis and Machine Intelligence*, vol. 24, no. 7, pp. 905-919, 2002.

[6] T. Lindberg, “Edge Detection and Ridge Detection with Automatic Scale Selection”, *Proceedings of IEEE conference on Computer Vision and Pattern Recognition (CVPR-96)*, San Francisco,USA,18-20 Jun, pp. 465-470, 1996.

[7] Y. Wang and J.K. Hu and F. Han, “Enhanced gradient-based algorithm for the estimation of fingerprint orientation fileds”, *Elsevier Journal of Applied Mathematics and Computation*, pp. 823-833, 185,2007.

[8] Z. Hou and W. -Y. Yan and Y. Wand, “A Review on fingerprint Orientation Estimation”, *Journal of Security and Communication Networks*, John wiley and Sons Ltd., Jun 2010.

[9] L. Liu and T. S. Dai, “A Reliable fingerprintg Orientation Estimation Algorithm”, *Journal of Information Science and Engineering*, vol. 27,no. 1, pp. 353-368, 2011.

[10] J. Sampo, J. Takalo, S. Siltanen, M. Lassas, A. Miettinen, and J. Timonen, “Curvelet-based method for orientation estimation of particles”, *http://www.siltanen-research.net/Orientation.pdf*, submitted manuscipt.

[11] T. Enomae, Y. -H. Han and A. Isogai, “Nondestructive determination of fiber orientation distribution of paper surface by image analysis”, *Nordic Pulp and Paper Research Journal*, Vol. 21, no. 2, pp. 253-259, 2006.

[12] T. Lindberg, “Scale-Space for discrete signals”, *PAMI*, Vol. 12, no. 3, pp. 234-254, March 1990.

[13] T. Lindberg, “Feature detection with automatic scale selection”, *International Journal of Computer Vision*, Vol. 30, no. 2, pp. 77-116, 1998.

[14] T. Lindberg, “Edge detection and ridge detection with automatic scale selection”, *International Journal of Computer Vision*, Vol. 30, no. 2, pp. 117-154, 1998.

[15] P. Perona, “Orientation diffusion”, *IEEE Transactions on Image Processing*, Vol. 7, no. 3, pp. 457-467, March 1998.

[16] B. Jahne, “Digital Image Processing”, *Springer-Verlag Publications, 6th Edition*, 2006.